Aryl Ether Dendrimers with an Interior Metalloporphyrin Functionality as a Spectroscopic Probe: Interpenetrating Interaction with Dendritic Imidazoles

Yoriko Tomoyose, Dong-Lin Jiang, Ren-Hua Jin, Takuzo Aida,* Takashi Yamashita,† and Kazuyuki Horie†

Department of Chemistry and Biotechnology, Graduate School of Engineering, The University of Tokyo, Hongo, Bunkyo-ku, Tokyo 113, Japan

Eiji Yashima‡ and Yoshio Okamoto‡

Department of Applied Chemistry, Faculty of Engineering, Nagoya University, Furo-cho, Chikusa-ku, Nagoya 464-01, Japan

Received April 17, 1996
Revised Manuscript Received May 14, 1996

Recent progress in the synthesis of dendritic molecules has provided a new methodology for molecular architecture to build up globular-shaped, hyperbranched macromolecules of nanoscopic size.[1,2] By reference to the chemistry of micellar aggregates, most studies to date focus attention on the functionalization of the exterior surface of dendrimers, but examples of core-functional dendrimers are only very limited.[3] Recently, we have reported the first example of a dendritic molecule having an interior metalloporphyrin functionality, the zinc porphyrin covalently linked to aryl ether dendritic arrays (L*n*PZn, *n* [number of aryloxy layers] = 1−4),[4−6] by Fréchet's convergent approach.[7] The interior zinc porphyrin functionality is usable as a spectroscopic probe. Herein we report results of a spectroscopic investigation on the interior properties of the dendritic zinc porphyrins, L*n*PZn (n = 1−5) and *p*-L5PZn, and wish to highlight their *interpenetrating* interaction with dendritic imidazoles (L*n*Im: n = 1, 2, and 4).

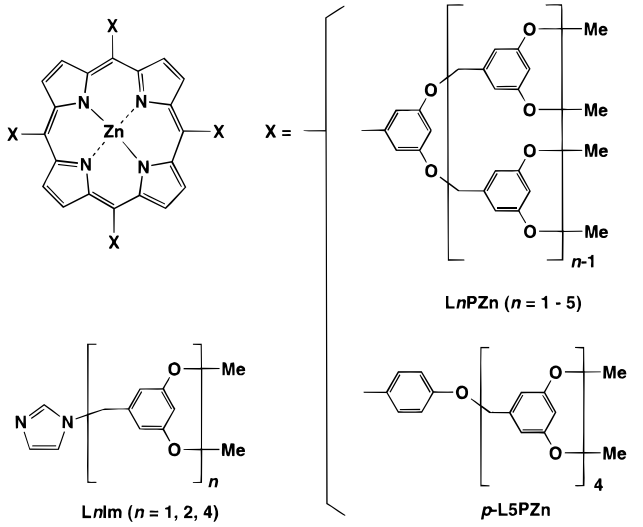

L5PZn[8] and *p*-L5PZn[9] were newly synthesized in a manner similar to that for L*n*PZn (n = 1−4).[4] Computer-generated molecular structures of L*n*PH_2[10] suggest that the morphology of the dendrimer framework stepwise changes from "open" (n = 1−3) to "semiclosed" (n = 4) to "closed" (n = 5) as the number of generations is increased, and the highest-generation L5PH_2 (Figure 1) takes a near-globular shape in diameter of approximately 5 nm. On the other hand, *p*-L5PZn takes a more open architecture than L5PZn, and is rather close to lower-generation L4PZn, since the dendritic arrays are attached to the *para* positions of the phenyl substituents on the interior zinc porphyrin skeleton. In the absorption spectra in CH_2Cl_2, the Soret bands of L*n*PZn (n = 2−5) were red-shifted from that of L1PZn (421.3 nm), and this tendency progressed as the number of generations was increased.[11] In particular, the Soret band wavelength of the highest-generation L5PZn in CH_2Cl_2 ($\lambda_{Soret}[CH_2Cl_2]$: 427.0 nm) was very close to that in 1,3-dimethoxybenzene (DMB), a monomeric model of the dendritic arrays (λ_{Soret}[DMB]: 427.7 nm), whereas those of L1PZn in these two solvents were considerably different from each other ($\Delta\lambda_{Soret}$ = 6.3 nm) (Figure 2, ■). Thus, in good correlation with the computational simulation, the encapsulation of the zinc porphyrin functionality by the dendrimer framework is almost accomplished for L5PZn. It is also worth noting that $\Delta\lambda_{Soret}$ for *p*-L5PZn was 2.1 nm, which is definitely larger than that for L5PZn (0.7 nm) but comparable to

† Responsible for fluorescence lifetime measurements.
‡ Responsible for molecular modeling studies.

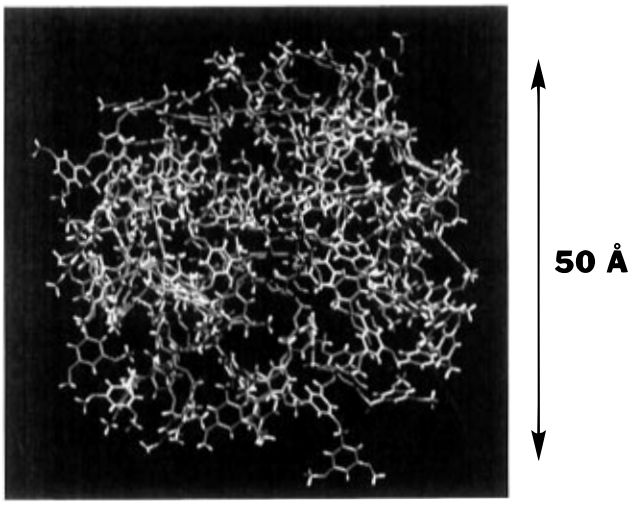

Figure 1. A wire-frame representation of a computer-generated molecular structure of L5PH_2.

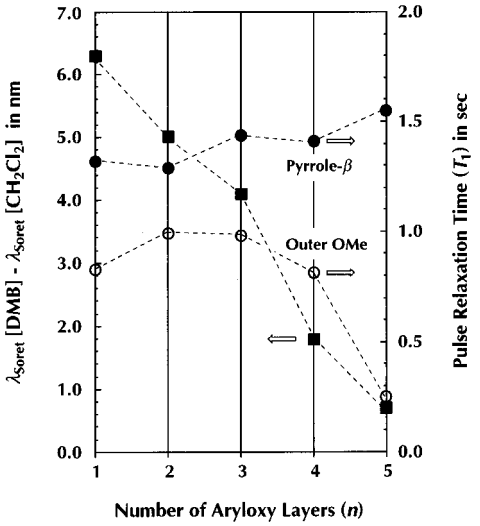

Figure 2. Differences in Soret band wavelengths (■) of L*n*PZn (n = 1−5) in 1,3-dimethoxybenzene (λ_{Soret}[DMB]) and CH_2Cl_2 ($\lambda_{Soret}[CH_2Cl_2]$), and ^{1}H NMR pulse relaxation times (T_1, ● and ○) of L*n*PH_2 (n = 1−5) in $CDCl_3$ at 20 °C.

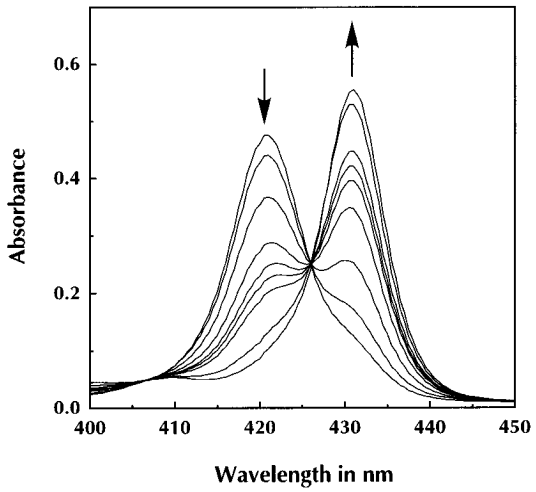

Figure 3. Spectral change in the Soret band absorption of L1PZn (7.1 μM) in CH_2Cl_2 at 20 °C upon titration with L4Im (0, 0.14, 0.35, 0.56, 0.70, 1.05, 1.75, 3.50, 10.50 mM).

that for lower-generation L4PZn (1.9 nm), indicating that the interior environments of *p*-L5PZn and L4PZn are similar to each other.

The L*n*PZn family upon excitation at the Soret band in MeCN emitted fluorescences at 604 and 659 nm.[4] A time-resolved fluorescence study[12] showed single-exponential decay profiles for L*n*PZn (n = 1, 4, and 5), where quite normal singlet lifetimes (1.6−1.7[±0.1] ns) were observed irrespective of the number of generations. Thus, the singlet excited state property of the zinc porphyrin functionality is not affected by the encapsulation with dendritic arrays. In connection with the observation, ^{1}H NMR pulse relaxation time (T_1) measurements of L*n*PH_2 (n = 1−5) in $CDCl_3$ (Figure 2) indicated that the conformational motion of the porphyrin skeleton (●) remains virtually intact upon increment of the number of generations, whereas the MeO groups (○) on the exterior surface become less mobile.[2a]

With all the above spectroscopic profiles in mind, the possibility of *interpenetrating* interaction between dendrimers was investigated using 1-dendritic imidazoles (L*n*Im, n = 1, 2, and 4). Figure 3 shows a typical example of the spectral change at the Soret region of L1PZn upon titration with L4Im in CH_2Cl_2 at 20 °C. Likewise, in every combination of L*n*PZn and L*n*Im, the absorption spectra of L*n*PZn upon addition of L*n*Im changed with clear isosbestic points. In each case, the plots of $\ln[(A_{obsd} - A_{[LnIm]=0})/(A_{[LnIm]=\infty} - A_{obsd})]$[13] versus ln[L*n*Im] gave a straight line with a slope close to unity (correlation factor: 0.98−0.99), indicating one-to-one complexation between L*n*PZn and L*n*Im. As expected, the binding constants (K) evaluated (Figure 4A) are obviously smaller as L*n*PZn and L*n*Im are larger. In good correlation with the spectral profile (■) in Figure 2, a notable gap in binding constant was observed between L3PZn and L4PZn. The highest-generation L5PZn exhibited an extremely low affinity toward the largest L4Im, where the observed binding constant (K = 2.4 × 10^2 M^{-1}) was merely 1/150 that of L1PZn toward L4Im and 1/5.8 that of L5PZn toward L1Im. On the other hand, *p*-L5PZn, bearing larger dendritic arrays than L4PZn, exhibited binding constants comparable to those of L4PZn, again indicating a more open architecture of *p*-L5PZn than L5PZn. Of further interest to note here is that the binding constants toward L2Im and L4Im relative to those toward L1Im (K_{LnIm}/K_{L1Im}, Figure 4B) showed upward-convex dependencies

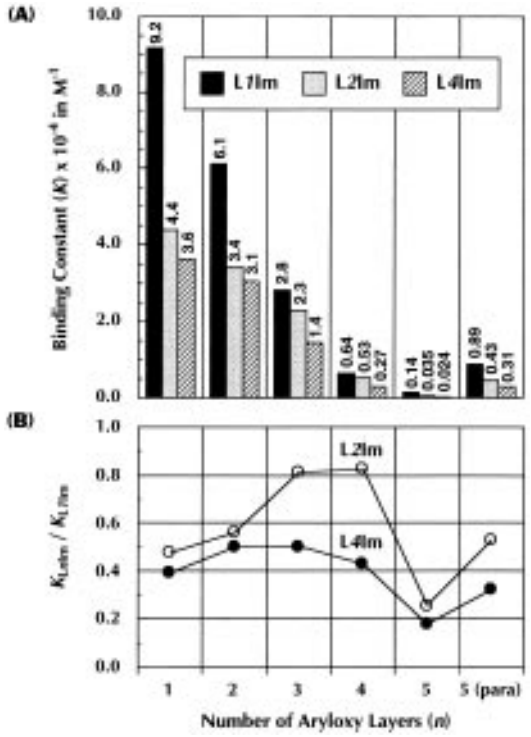

Figure 4. Spectrophotometric titration of L*n*PZn (n = 1−5) and *p*-L5PZn with dendritic imidazoles (L*n*Im, n = 1, 2, and 4) in CH_2Cl_2 at 20 °C: (A) Binding constants (K) and (B) ratios of binding constants toward L*n*Im (n = 2 and 4) to those toward L1Im (K_{LnIm}/K_{L1Im}).

on the number of generations of L*n*PZn, suggesting that a van der Waals attractive force (complementarity) is operative in competition with the size-exclusion force.

In summary, by using the interior metalloporphyrin functionality as a spectroscopic probe, we have shown a structure−interior property relationship for an aryl ether dendrimer family and evaluated for the first time the *interpenetrating* interaction between dendrimer molecules. Further studies on biomimetic applications of dendritic metalloporphyrins are in progress.

Acknowledgment. The present work was sponsored by Grant-in-Aid on Priority Area Research "Photoreaction Dynamics" from the Ministry of Education, Science, Culture, and Sports, Japan. The authors also thank Mr. T. Nirasawa of Bruker Japan Co., Ltd., for MALDI-TOF-MS measurements.

Supporting Information Available: Syntheses and analytical data of dendritic benzyl bromides (L*n*Br, n = 1−4), dendritic benzyl alcohols (L*n*OH, n = 2−4), L*n*PH_2/L*n*PZn (n = 1−5), *p*-L5PH_2/*p*-L5PZn, and L*n*Im (n = 1, 2, and 4), method for molecular modeling calculations of L*n*PH_2 (n = 1−5) and *p*-L5PH_2, and experimental procedures and results of titration of L*n*PZn (n = 1−5) and *p*-L5PZn with L*n*Im (n = 1, 2, and 4) (15 pages). This material is contained in many libraries on microfiche, immediately follows this article in the microfilm version of the journal, can be ordered from the ACS, and can be downloaded from the Internet; see any current masthead page for ordering information and Internet access instructions.

References and Notes

(1) Recent reviews: (a) Fréchet, J. M. J. *Science* **1994**, *263*, 1710. (b) Tomalia, D. A. *Adv. Mater.* **1994**, *6*, 529.

(2) Recent examples: (a) Jansen, J. F. G. A.; Ellen, M. M.; de Brabander-van den Berg, E. M. M.; Meijer, E. W. *Science* **1994**, *266*, 1226. (b) Hawker, C. J.; Farrington, P. J.; Mackay, M. E.; Wooley, K. L.; Fréchet, J. M. J. *J. Am. Chem. Soc.* **1995**, *117*, 4409. (c) Newkome, G. R.; Güther, R.;

Moorefield, C. N.; Cardullo, F.; Echegoyen, L.; Pérez-Cordero, E.; Luftmann, H. *Angew. Chem., Int. Ed. Engl.* **1995**, *34*, 2023. (d) Ottaviani, M. F.; Cossu, E.; Turro, N. J.; Tomalia, D. A. *J. Am. Chem. Soc.* **1995**, *117*, 4387.

(3) Examples of core-functional dendrimers: (a) Hawker, C. J.; Wooley, K. L.; Fréchet, J. M. J. *J. Am. Chem. Soc.* **1993**, *115*, 4375. (b) Wooley, K. L.; Hawker, C. J.; Fréchet, J. M. J.; Wudl, F.; Srdanov, G.; Shi, S.; Li, C.; Kao, M. *J. Am. Chem. Soc.* **1993**, *115*, 9836. (c) Newkome, G. R.; Moorefield, C. N.; Keith, J. M.; Baker, G. R.; Escamilla, G. H. *Angew. Chem., Int. Ed. Engl.* **1994**, *33*, 666.

(4) Jin, R.-H.; Aida, T.; Inoue, S. *J. Chem. Soc., Chem. Commun.* **1993**, 1260.

(5) Sadamoto, R.; Tomioka, N.; Aida, T. *J. Am. Chem. Soc.* **1996**, *118*, 3978.

(6) An ether−amide dendritic zinc porphyrin synthesized by the divergent approach has more recently been reported in: Dandliker, P. J.; Diederich, F.; Gross, M.; Knobler, C. B.; Louati, A.; Sanford, E. M. *Angew. Chem., Int. Ed. Engl.* **1994**, *33*, 1739.

(7) Hawker, G. J.; Fréchet, J. M. J. *J. Am. Chem. Soc.* **1990**, *112*, 7638.

(8) UV−vis (CH_2Cl_2): λ_{max} (log ϵ) 427.0 (5.63), 516.0, 552.0, 590.5.

(9) UV−vis (CH_2Cl_2): λ_{max} (log ϵ) 426.5 (5.67), 553.0, 593.5, 686.0.

(10) By molecular mechanics and dynamics calculations with the Dreiding force field as implemented in Cerius^2 software running on an Indigo2 Extreme graphics workstation.

(11) Utilization of cyclic voltammetry for evaluation of the degree of encapsulation has been reported in refs 2c and 6.

(12) Time-resolved fluorescence measurements were performed on a Horiba NAES-550 single-photon-counting apparatus equipped with a pulsed hydrogen lamp as a light source. Emissions upon excitation at the Soret band of L*n*PZn with an interference filter (Toshiba KL-42) and a cutoff filter (Toshiba UV-38) were collected. The decay curves were satisfactorily analyzed by $I_f(t) = A \exp(-t/\tau)$.

(13) $A_{[LnIm]=0}$ and $A_{[LnIm]=\infty}$ are the Soret band absorbances of L*n*PZn without L*n*Im and with a large excess of L*n*Im, respectively.

MA960575+